THERMAL AND STRESS ANALYSIS IN Nd:YAG LASER ROD WITH DIFFERENT DOUBLE END PUMPING METHODS

by

Khalid S. SHIBIB*[*], *Mohammed A. MINSHID, and Nebras E. ALATTAR

Department of Laser and Optoelectronics Engineering, University of Technology, Baghdad, Iraq

Original scientific paper
UDC: 621.375.826:536.24
DOI: 10.2298/TSCI101201004S

In this work, the finite element analysis has been used to predict the temperature distribution in Nd:YAG laser rod; double end-pumped by two methods Gaussian or top hat beam. The rod is cooled by water passing through annular, which surrounds the active media. The temperature distribution has been used to predict numerically, the nodal displacements, strain and stress based on the principle of virtual work. The main task is to determine the temperature distribution in Nd:YAG laser rod, the subsequent value and location of maximum tensile hoop stress associated with the two types of the double end pumping for different absorption power. Some conclusions are obtained; as the radius pumping ratio increases the location of maximum hoop stress will move toward the periphery and vice-versa. Small reduction is observed in the location of maximum hoop stress when pumping method change from the top-hat beam to Gaussian beam, especially at low radius pumping ratio and high absorption power. Top hat beam end pumping will cause more intense tension hoop stress at the facets of the rod than that of Gaussian beam even the later may produce high center temperature. This work may be important for designer while choosing the type of pumping, maximum produced tensile hoop stress and its location, especially when hoop stress is ultimate.

Key words: *Nd:YAG laser rod, thermal distribution, stress distribution, finite element analysis, double end pumping, high laser power*

Introduction

The increasing demand on high laser power in industries required deep insight in the portion of pump radiation absorbed by laser media that converts to heat. Heat may be one of the most limitations in increasing power of the laser systems. It may cause thermal stress, stress birefringence and thermal lens effect which may degrade the optical properties of the laser medium, reduce the laser output and beam quality and even lead to medium break [1], so efficient heat removal is required. The reductions of the thermal effects that are caused by the temperature gradients across the active area of the laser medium usually dominate design con-

* Corresponding author; e-mail: assprofkh@yahoo.com

siderations for high-average-power systems. Great interest in the end pumping of solid-state laser has developed; because it allows efficient fundamental-mode operation [2]. The modeling of the thermal problem in the laser medium has been an important issue as from the first days of laser science and technology. Today, with the availability of fast computers, the modeling is most often made by numerical methods [2, 3]. These methods are reliable and the codes can be modeled with an efficient procedure as the science of different numerical method such as finite element method is well established where a different temperature dependent properties, varying boundary conditions and inside heat generation can be imposed. Numerical modeling remains however a rather long exercise and suffers the usual limitation that there is no insurance of the correctness of the solution so comparisons with the restricted analytical solution, experimental data or previously published work are a matter of importance. Although the analytical treatment of the thermal problem has many limitations in dealing with non-uniform shapes, temperature dependent physical properties and boundary conditions, it is of interest to compare their result by the numerical result of a same physical domain and boundary conditions. The analytical treatment of the thermal problem is often based on the assumption of uniform internal heat generation along the radial and longitudinal co-ordinates, as in the case of Nd:YAG rod, pumped transversely by diodes. This is a reasonable assumption in the case of side pumping [1]. However, a comparison between the analytical treatments of a homogeneous structure with the numerical analysis of the same structure in the presence of a more realistic heat distribution is made so that, when it has revealed small differences in the resulting temperature distributions and the subsequent thermal stress, it will verify the numerical solution.

In this work, a finite element program is created to predict the temperature distribution in Nd:YAG laser rod that double end pumped by either Gaussian or top hat beam (this rod is cooled by water surrounding the active media) from which the nodal displacements, strain and stress are obtained also the locations and values of the maximum tensile hoop stress result from the two types of pumping at different absorption power and radius pumping ratio are tested.

Theory

Partial differential equation

In laser rod, the thermal behavior can be covered by the steady-state axis-symmetry partial differential equation that modeled the axis-symmetry domain of laser rod [1]:

$$\frac{1}{r}\left[k\frac{\partial}{\partial r}\left(r\frac{\partial T}{\partial r}\right)\right]+k\frac{\partial^2 T}{\partial z^2}+\dot{Q}(r,z)=0 \tag{1}$$

and the temperature dependent thermal conductivity equation of Nd:YAG laser rod is extracted from [4] which can be written as:

$$k=1.9\cdot 10^8[\ln(5.33T)^{-7.14}]-\frac{33100}{T} \tag{2}$$

The laser rod, fig. 1, has a diameter D_i of 9.5 mm and its length (L) is 20 mm. The inside diameter D_o of the cooling passage is 13.5 mm. Furthermore, adiabatic boundary condi-

tions are assumed at the rod surface ends and at the outer surface of the water passage. The water mass flow rate that has been used to cool the laser rod is 0.1 kg/s.

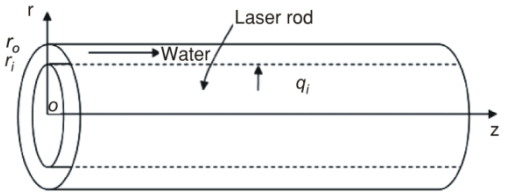

Figure1. Schematic diagram for laser rod and water passage

Convection boundary condition

Convection boundary conditions are assumed at the longitudinal surface where a concentric tube may well model the situation:

$$q_i = hA_i(T_s - T_\infty) \tag{3}$$

where the turbulent heat transfer coefficient denote by *h*, can be obtained by using a simple realistic procedure [1]:

$$h = 10.47 \cdot 10^{-3} \frac{\left(\frac{D_0}{D_i}\right)^{0.53}}{(D_o - D_i)(D_o + D_i)^{0.8}} f^{0.8} \tag{4}$$

The average bulk temperature of the cooling fluid can be obtained by applying the following heat equation:

$$T_{\text{final}} = T_{\text{in}} + \frac{2\pi r_i L q_i}{\dot{m} c_p} = T_{\text{in}} + \frac{2P\eta}{\dot{m} c_p} \tag{5}$$

Assuming the maximum tested absorption power is P = 100 W and a heat factor η is 0.32 for this type of rod, inlet temperature of 25 °C then T_{final} is not exceed 25.15 °C as obtained from eq. (5). The enviermental temperature used in the equation of convection heat transfer is assumed to be the average of these temperatures.

Heat generation inside laser rod

Two methods of pumping are tested; Gaussian and Top-hat beam distribution which caused a heat generation through the laser medium also it is assumed that the same power is absorbed in two types of pumping. A realistic heat source density is assumed, which has the same shape as the pump light absorption. For Gaussian beam distribution, the heat generation through the laser medium is [5]:

$$\dot{Q}(r,z) = \frac{2Q\exp\left(\frac{-2r^2}{w_o^2}\right)\exp(-\mu z)}{\pi w_o^2[1-\exp(-\mu L)]} \tag{6}$$

Here $Q = \eta P$, μ = 3.5 cm^{-1}, and for uniform power distribution through the beam (Top-hat), the heat generation through the laser medium is [6]:

$$\dot{Q}(r,z)=\frac{Q\mu\exp(-\mu z)}{\pi a^2[1-\exp(\mu L)} \tag{7}$$

This equation is applied through laser rod as long as the radius is equal or less than the radius of the pumping beam denoted by *a*, and the heat generation is vanished as the radius is grater than the beam radius.

Finite element formulation

Thermal analysis

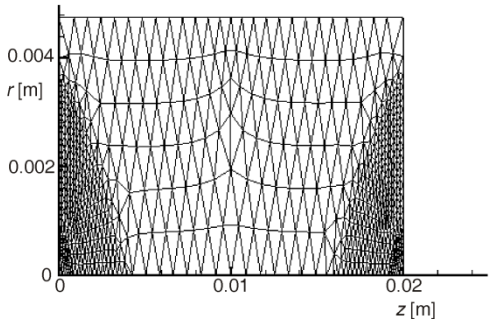

Figure 2. Studied domain and used mesh

Equation (1) is solved using the weak formulation and Galerkin procedure [7]. A total number of 1184 triangular elements and 653 nodes are generated follow a special grid model, see fig. 2. High concentrated node near severe gradient boundary and inside conditions is applied to ensure accurate non-osculating result. A computer program is created, which follows the procedure of predicting the temperature distribution through the domain and the subsequent nodal displacement, strain, and thermal stress in the studied region. The mesh shown in fig. 2 that has been used in the thermal analysis is also used in the mechanical analysis. An iterative procedure is followed to predict the temperature distribution based on temperature dependent thermal conductivity, which may reduce the error caused by fixing this property.

Thermal stress analysis

The temperature gradients generate mechanical stresses in the laser rod since the hotter inside volume is constrained from expansion by the cooler outer zone. To obtain the thermal stress distribution, it is assumed that the laser rod reaches thermal equilibrium at the steady-state thermal condition. Therefore, stress components (σ_{rr}, σ_{zz}, $\sigma_{\theta\theta}$, τ_{rz}) are calculated at this steady-state condition. During power pumping, the heating is localized in laser rod and, therefore, large temperature variations occur over a small region. Owing to this temperature gradient, large thermal stresses are generated in laser rod, which can lead to defect the material such as the formation of cracks and the fractures in the material.

To develop a finite element procedure for the stress computation, the principle of virtual work is used. According to this principle, the equilibrium of anybody under loading requires that for any compatible small virtual displacements imposed on the body in its state of equilibrium, the total virtual internal work or strain energy (δU) is equal to the total virtual external work due to the applied thermal loads (δV), *i. e.* $\delta U = \delta V$. For the static analysis of problems having linear geometry and thermo-elastic material behavior, one can derive simultaneous equations that relate the global displacement vector and the global force vector. The standard procedure is clearly followed by many references [8-10], then the nodal displacements, thermal strains and the subsequent thermal stresses can be obtained. As the compres-

sive fracture strength is 5-6 times higher than tensile strength for laser material, it is generally admitted that fracture occurs when the maximum tensile hoop (tangential) stress $\sigma_{\theta\theta}$ anywhere in the rod exceeds its yielding tensile stress, which is found to be in a range of 124-255 MPa [3]. The later depends on both the fracture toughness of the material and on its surface flatness. These aspects have been studied in detail in [11-13]. A general acceptable value for fracture tensile strength of Nd:YAG material, as suggested in [2], is equal to 137.88 MPa.

Some note is required on the thermal expansion coefficient of Nd:YAG laser rod which is treated as temperature-dependent and can be expressed as [14]:

$$\alpha(T) = -1.78 \cdot 10^{-6} + 3.3 \cdot 10^{-8} T \tag{8}$$

The present study uses a weighted-average value of α, such that the reference temperature and current temperature are involved to get the mean average value of α [14], assume that the reference temperature is the initial temperature which is taken to be that of the inlet water temperature.

Validation

Firstly, a comparison is made between the program of this work and an analytical solution for temperature distribution in laser rod derived by Li *et al*. [15]. High restrictions are used to solve the same physical domain (*i. e*. insulated end sides, constant thermal properties, constant heat generation through laser rod) and a good agreement is found so that a maximum difference of no more than 0.5% has been found, which may verify the created finite element program used in this paper. The obtained solution using the current program is shown in fig. 3. Radial and longitudinal displacements, strains and stresses component are tested and a good agreement has been reached especially at the center cross-section of the rod, the difference may not exceed 1% in the worst case. Although to increase confidence with the numerical solution, results of this program have been compared with that of Pfistner *et. al*. [2] for their physical domain, boundary and inside conditions and very near by results are found including the optical path difference.

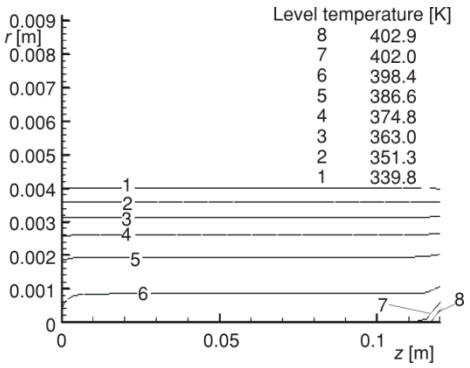

Figure 3.Temperature distribution through laser rod using finite element solution

For a paraxial coherent beam propagating in the z-direction, the optical path difference (*OPD*) is given in [12]. By neglecting the contribution from thermal stress induced birefringence which is small for most cases [2], the *OPD* can be expressed as for multiple passages in laser rod as:

$$OPD(r) = 2\left[\int_L \frac{\partial n}{\partial T} T(r,z)\mathrm{d}z + \int_L n\varepsilon_{zz}\mathrm{d}z\right] \tag{9}$$

Even this property is well known in the optical science, its determination is based on thermal and mechanical analysis. A comparison is made between its value, which obtained

from experimental and theoretical analysis. This comparison may verify the method of analysis and the obtained result. This validation is very important, and gives the required confidence to the created program (thermal and mechanical analysis). The result from the created program has been tested with that of [2] for the center to edge *OPD* and it is found to be in order of 2.215 μm, which is very near to a value of 2.2 μm obtained experimentally [2] (*i. e.* 0.6% allowance).

Results and discussion

With its large facilitates, the numerical solution can be used to solve large varieties of both boundary conditions and types of heat generation inside the laser rod, which can converge to real conditions. After the computer program has been verified, which gives the required confidence to the created finite element analysis, the program is used to predict the temperature distribution and the subsequent displacements, strain, and stress at both types of the double end pumping for top hat and Gaussian pumping at different absorption power level. The nodal temperature distribution is used to predict radial and axial displacement where zero radial displacement boundary condition is imposed at the axis of symmetry then radial, hoop, longitudinal, and shear strain are obtained from which the equivalent stress can be calculated. The ratio of pumping radius to the outer laser rod radius which is known as the radius pumping ratio (*PR*) can be written mathematically as:

$$PR = \frac{r_{\mathrm{p}}}{r_{\mathrm{i}}} \tag{10}$$

This ratio *PR* is tested for different values say 1/2, 1/3, and 1/4. Firstly, a radius *PR* of 1/3 and an absorbed power of 80 W are tested. The temperature distribution at both types of pumping is shown in fig. 4. The temperature difference between the same end centers reaches 22.6 °C. Gaussian pumping seems to have the higher temperature distribution, especially at the center of ends, this is due to intense absorption power there. The rod core, which has a higher temperature than the periphery, is restrained from expanding by the outer portions of the rod, which may cause compressive hoop stress in the central portion of the rod while the outer portions of the rod are in tension, see fig. 5.

Studying the difference between Gaussian and top hat pumping shows that the former will cause high compressive hoop stress at the rod core more than that for later, this is due to concentrated power at the center portion of the rod which leads to high temperature, high displacements, high strain there, and consequently, high compressive stresses.

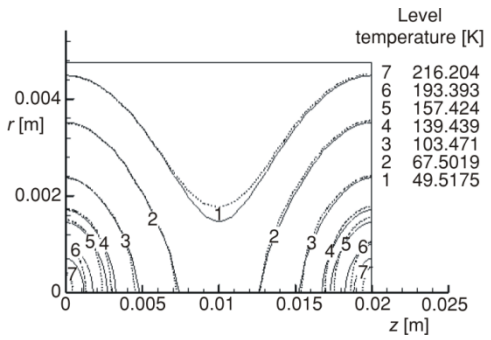

Figure 4. Temperature distribution at absorption power of 80 W, Pr = 1/3, absorption power from both end;
Solid line for Gaussian pumping , small dashed line for top hat, max. temperature at far end for Gaussian pumping is equal to 247.34 °C

In the top hat beam, due to uniform power distribution across its radius, which is not the case for Gaussian distribution, more intense tensile hoop thermal stress at the facets of laser rod is observed. This is obvious beyond the outer surface radius of the pumping (*i. e.* w_p for Gaussian and *a* for top-hat beam) comparing with Gaussian beam, see figs. 5(a) and (b). It shows the maximum tensile hoop stress that occurs at the facets of the rod where the top hat beam seems to produce more tensile hoop stress than Gaussian beam. Increasing the radius pumping ratio will dramatically reduce temperature distribution, and the subsequent displacement, strain and stress. This is due to the reduction in the intense of absorption power, fig. 6. It shows also that the maximum tensile hoop stress will increase as absorption power increases. The maximum tensile hoop stress for top hat beam seems to be larger than that for Gaussian beam even the maximum temperature is recorded at Gaussian pumping method, fig. 7.

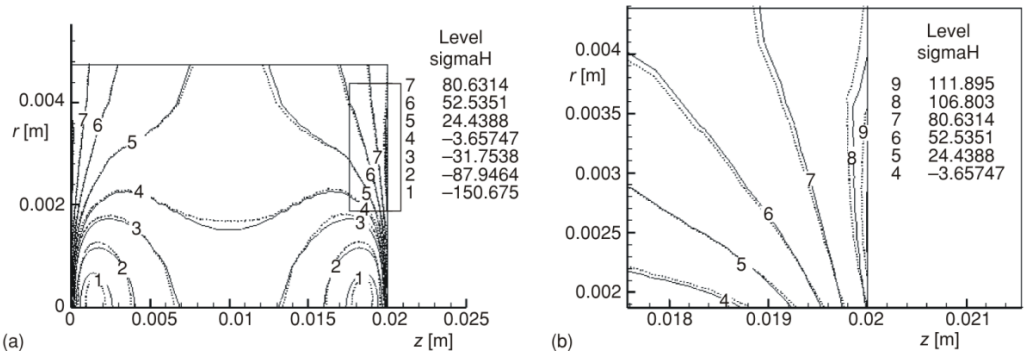

Figure 5. Contour of hoop stress in MPa with absorption power of 80 W from both end;
Solid line for Gaussian pumping, dashed line for top hat pumping (maximum hoop stress 114.6 MP), (b) is an enlarged view of the rectangle indicated in (a)

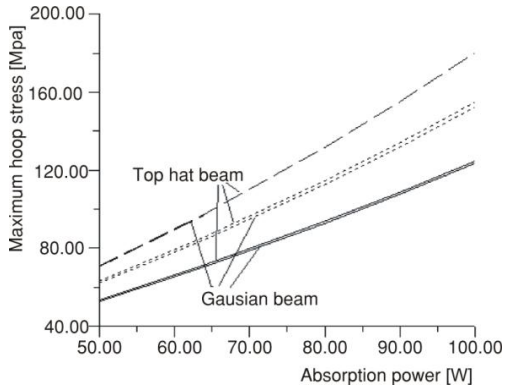

Figure 6. Variation of maximum tensile hoop stress with absorption power for different radius *PR*;
Solid for PR = 1/2, small dashed for PR = 1/3, long dashed for PR = ¼

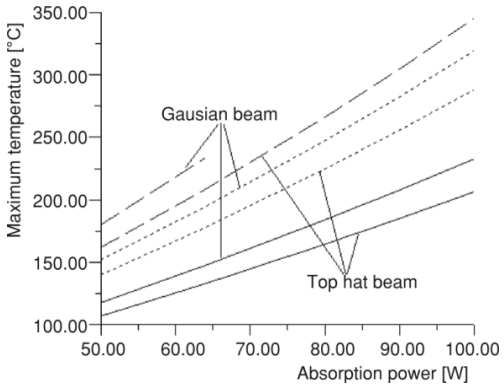

Figure 7. Variation in the maximum temperature occurs at the center of faces of rod;
Solid line for PR = 1/2, small dashed line for PR = 1/3, long dashed line for PR = 1/4

The location of maximum produced stress will move toward the periphery as the radius pumping ratio increase. This is clearly shown in fig. 8. Increasing the absorption power will increase the maximum hoop stress, and its location may move toward the center. As the

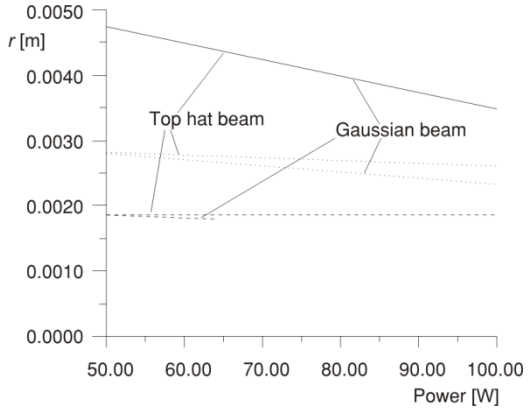

Figure 8. Variation in the location of maximum tensile hoop stress with absorption power; *Solid line for PR = 1/2, small dashed line for PR = 1/3, dashed line for PR = 1/4*

pumping method is changing from the top-hat beam to Gaussian, a margin reduction in the radius at which maximum tensile hoop stress occurs especially at low radius pumping ratio.

An interesting observation can be obtained. Type of pumping has a small effect on the change in the location of maximum tensile hoop stress, especially at low absorption power. Reducing the radius pumping ratio and increasing absorption power clarify that Gaussian beam have some decrease in radius at which maximum tensile hoop stress occurs comparing with that of the top-hat pumping beam. In [16], it was shown that Gaussian beam has thermal lensing that is a factor of 2 stronger than a top hat intensity distribution. So, some wisdom is necessary while design the laser system, reducing the thermal lensing by choosing the top hat may be limited by the highest hoop stress produced. These factors may be crucial as the density of the absorption power increase where the yield tensile hoop stress may be reached.

Conclusions

Some conclusions are obtained for double end pumping at the tested range of radius PR:

- As the radius *PR* increases the location of maximum hoop stress will move toward the periphery and vice-versa.
- Small reduction in radius is observed in the location of maximum hoop stress when pumping method change from the top-hat beam to Gaussian beam, especially at low radius *PR* and high absorption power.
- Top hat beam end pumping will cause more intense tension hoop stress than that of Gaussian beam even the later may produce high center temperature. Some wisdom is necessary in designing Nd:YAG laser system since Gaussian beam has a determinant effect of high thermal lensing.

Nomenclature

A – area, [m^2]
a – radius of top hat beam, [m]
c_p – water specific heat, [Jkg^{-1}K^{-1}]
D – diameter, [m]
f – volume flow rate [cm^{3}s^{-1}]
h – convection heat transfer coefficient, [Wm^{-2}K^{-1}]
k – thermal conductivity, [Wm^{-1}K^{-1}]
L – rod length, [m]
$\dot{m}$ – mass flow rate, [kgs^{-1}]
n – refractive index, [–]
P – absorption power, [W]
Q – absorbed power, [W]
$\dot{Q}$ – heat generation, [Wm^{-3}]
q – convective heat, [W]
r – radial domain, [m]
T – temperature, [K]
w_o – radius of Gaussian beam, [m]
z – longitudinal domain, [m]

Greek symbols

α – thermal expansion coefficient, [mK^{-1}]
ε – strain, [–]
η – heat factor, [–]
μ – absorption coefficient, [m^{-1}]
σ – stress, [Pa]
τ_{rz} – shear strain, [Pa]

Subscripts

i – inner
o – outside
p – pumping
s – surface
∞ – environmental

References

[1] Koechner, W., Solid-State Laser Engineering, 6th ed., Springer Series, in Opt. Sci., New York, USA, 2006
[2] Pfisther, C., *et al*., Thermal Beam Distortions in End-Pumped Nd:YAG, Nd:GSGG, and Nd:YLF Rods, *IEEE Journal of Quantum Elelectronics, 30* (1994), 7, pp. 1605-1614
[3] Steve, C. T., *et al*., Scaling CW Diode-End Pumpued Nd:YAG Laser to High Average Powers, *IEEE Journal of Quantum Electronics, 28* (1992), 4, pp. 997-1008
[4] Brown, D. W., Nonlinear Thermal and Stress Effects and Scaling Behavior of YAG Slab Amplifiers, *IEEE Journal of Quantum Electronics, 34* (1998), 12, pp. 2393-2402
[5] Frauchiger, J., Peter, A., Heinz P. W., Modeling of Thermal Lensing and Higher Order Ring Mode Oscillation in End-Pumped CW Nd:Lasers, *IEEE Journal of Quantum Electronics, 28* (1992), 4, pp. 1046-1056
[6] Ananada, K. C., Temperature and Thermal Stress Scaling in Finite-Length End-Pumped Laser Rods, *IEEE Journal of Quantum Electronics, 28* (1992), 4, pp. 1057-1069
[7] Lewis, R. W., *et al*., The Finite Element Method in Heat Transfer Analysis , John Wiley & Sons Ltd., Chichester, UK, 1996
[8] Rao, S. S., The Finite Element Method in Engineering, 4th ed., Elsevier Science and Technology Books, London, 2004
[9] Sunar, M., Yilbas, B. S., Boran, K., Thermal and Stress Analysis of a Sheet Metal in Welding, *Journal of Materials Processing Technology, 172* (2006), 1, pp. 123-129
[10] Khan, o. U., Yilbas, B. S., Laser Heating of Sheet Metal and Thermal Stress Development, *Journal of Materials Processing Technology, 155-156* (2004), part. 2, pp. 2045-2050
[11] Marion, J., Strengthened Solid-State Laser Materials, *Applied Physics Letters, 47* (1985), 7, pp. 94-96
[12] Marion, J., Fracture of Solid-State Laser Slabs, *Journal of Applied Physics, 60* (1986), 1, pp. 69-77
[13] Marion, J., Appropriate Use of the Strength Parameter in Solid-State Slab Laser Design, *Journal of Applied Physics, 62* (1987), 5, pp. 1595-1604
[14] Fan, T. Y., Daneu, J. l., Thermal Coefficients of the Optical Path Length and Refractive Index in YAG, *Applied Optics, 37* (1998), 9, pp. 1635-1637
[15] Li, Z., *et al*., A Study of Axisymmetric Thermal Strain in a Laser Rod with Longitudinal Temperature Rise, *Applied Thermal Engineering, 29* (2009), 14-15, pp. 2927-2934
[16] Clarkson, W. A., Felgate, N. S., Hanna, D. C., OSA TOPS., Vol. 19, Advanced Solid-State Lasers, (Eds. W. Rosenberg., M. M. Feijer), Opt. Soc. Am., Washington, 1998

Paper submitted: July 8, 2010
Paper revised: January 21, 2011
Paper accepted: January 23, 2011